

Citation for published version:

Vijayakumar, R, Akehurst, S, Liu, Z, Reyes Belmonte, M, Brace, C, Liu, D & Copeland, C 2019, 'Design and Testing a Bespoke Cylinder Head Pulsating Flow Generator for a Turbocharger Gas Stand', *Energy*, vol. 189, 116291, pp. 1-16. https://doi.org/10.1016/j.energy.2019.116291

DOI:

10.1016/j.energy.2019.116291

Publication date: 2019

Document Version
Peer reviewed version

Link to publication

Publisher Rights CC BY-NC-ND

University of Bath

Alternative formats

If you require this document in an alternative format, please contact: openaccess@bath.ac.uk

General rights

Copyright and moral rights for the publications made accessible in the public portal are retained by the authors and/or other copyright owners and it is a condition of accessing publications that users recognise and abide by the legal requirements associated with these rights.

Take down policy

If you believe that this document breaches copyright please contact us providing details, and we will remove access to the work immediately and investigate your claim.

Download date: 08. Mar. 2023

DESIGN AND TESTING A BESPOKE CYLINDER HEAD PULSATING FLOW GENERATOR FOR A TURBOCHARGER GAS STAND

R Vijayakumar a, S Akehurst a, Z Liu a, M A Reyes-Belmonte b, CJ Brace a, D Liu a, C Copeland a*

^a Department of Mechanical Engineering, University of Bath, Bath, BA2 7AY, Somerset, United Kingdom
 ^b IMDEA ENERGY Institute, Avda. Ramón de la Sagra, 3 Parque Tecnológico de Móstoles, E-28935, Móstoles, Madrid, Spain

ABSTRACT

Most turbocharger gas stands are designed to map performance under steady flow conditions. However, when connected to an internal combustion engine (ICE), the turbine is exposed to pulsatile flow. In order to enable a full analysis of the unsteady flow and turbocharger performance, it is crucial to quantify unsteady flow effects in the gas stand tests.

This paper presents the development and use of bespoke experimental hardware that aims to generate flows in a gas-stand with characteristics similar to that produced by an ICE. This is achieved using a specially modified cylinder head placed between the hot supply and the turbocharger. The device has been designed, manufactured and tested on the gas stand showing its usefulness to study the energy exchange between the engine and the turbine.

Testing a turbocharger where a cylinder is deactivated showed large changes in the instantaneous turbocharger speed, pressure and temperature profiles. These unsteady characteristics resulted in a change in the turbocharger behaviour. The insights into unsteady characteristics is expected to contribute to both engine calibration and turbocharger design. It also demonstrates the novelty of the approach in delivering a means to replicate hot, engine-like flow unsteadiness and thereby a wider, more representative data set.

KEYWORDS

Pulsating flow generator design, Turbocharger, gas stand, pulsation generator, unsteady flow, turbine map, compressor map, cylinder deactivation, turbine efficiency, compressor surge

Tel.: +44(0) 1225384551; E-mail address: C.D.Copeland@bath.ac.uk

1. INTRODUCTION

Turbocharger usage is becoming increasingly common to lower CO2 emissions [1] by improving the thermal efficiency of internal combustion engines [2] and thereby address future energy sustainability targets in both the transport and power generation sectors. Better fuel efficiency is supported by technological advancements such as the variable geometry turbine (VGT) [3], multiple stage turbocharging [4], hybrid turbocharging (also called electrically assisted turbocharging) [5], electrically driven compressor [6] and turbo compounding [7]. In addition, engine valve timing control is in widespread use supporting aggressive Miller cycle strategies and cylinder deactivation. Working together, these engine gas exchange and air supply systems work to maximise engine energy efficiency (thereby improving fuel sustainability) whilst reducing emissions. However, the advances in this area must be supported by more detailed engine and air path system data and informed by more accurate modelling tools. This paper aims to demonstrate a new system analysis tool used in a gas stand – a controlled laboratory for turbocharger testing. It also demonstrates the ability of this tool to provide new insights into the behaviour of the turbocharger when exposed to cylinder deactivation. This will demonstrate the importance of this experimental approach in achieving further engine efficiency improvements by enhanced data collection and modelling.

The 1D gas dynamic modelling tools speed engine development and hence find a wide usage in the automotive industry. These modelling approaches use steady state derived turbocharger maps obtained from conventional gas stands [8]. Conventional steady flow gas stands maps are obtained at 600° C and with a steady turbine inlet flow as specified in the SAE code [9]. This modelling approach adopts the classical quasisteady assumption to use the turbine map as a look-up table at each instance of time during the exhaust pulse [10], thus

^{*} Corresponding author. Department of Mechanical Engineering, University of Bath, Bath, BA2 7AY, Somerset, United Kingdom

predicting instantaneous behaviour based on the steady flow mapping data [11].

Gas stand measurements of the turbine are limited by the breadth of the loading available from the compressor (surge and choke limitations). In order to address the limited data on the turbine, extrapolation techniques [14] and mean value models [15] are used to predict the performance for the operating points outside the data map [16]. However, many of these models are based on the local empirical observation that do not involve any flow physics or are limited by the narrow data set [12]. Hence, the extrapolation can be unsatisfactory [17]. New advances in engine technologies are pushing the limits of operation for turbochargers to regions where having estimations of turbine efficiency gives the possibility to run reliable full engine simulations. In order to facilitate turbocharger modelling at off-design conditions, some physically-based extrapolation models have been proposed over the last few years [18].

To get a better knowledge of the turbine and compressor unsteady performance characteristics necessitates the capability to generate unsteady flow similar to on-engine conditions but on the turbocharger gas stand. Some researchers have demonstrated that turbocharger performance under pulsating flow conditions could be predicted from the steady map if extensive, good quality data beyond that typically captured was available [19]. This approach also requires a physically-based extrapolation methodology that utilizes turbocharger geometrical data and a heat transfer model [13]. However, the pulse generator presented in this paper could potentially simplify this modelling work by providing turbine and compressor maps that are closer to the typically operating regime on the engine. In addition, it provides the capability to characterize turbine and compressor performance in unsteady flows and thus, can contribute to improved aerodynamic designs.

Although the potential for such a pulsating flow facility is significant, there are a number of measurement difficulties that need to be addressed. In particular, quantifying unsteady turbine efficiency requires the ability to measure the time-resolved mass flow rate in a hot environment [20]. If the techniques to measure the instantaneous parameters are addressed, however, the potential to improve the representation of the turbo machinery in 1D models represents an important step forward. For example, reference [21] shows how a fully unsteady turbine map can be generating in a pulsating gas-stand that could potentially completely replace the steady-state map.

In this paper, a methodical approach to develop a pulsating flow generator is described through the use of 1D gas-dynamic models. The design of a pulse generator that utilizes a cylinder head was chosen in order to be able to replicate the most realistic pulse-train behaviour such as variable actuation and cylinder deactivation. A sample data set from such a study will be shown and discussed. In addition, an example data set studying

compressor surge under pulsating flow will also be shown and discussed.

2. BACKGROUND

Several methods that can produce pulsating flow in a turbocharger gas stand are described in the literature [22] [23] [24] [25]. The usage of diametrical slot rotating valves with a variable speed motor to generate pulsating flow reproduces engine-like flow. The pulse characteristics including mean value, amplitude, shape and frequency of the pressure pulse at the turbine inlet can be regulated by mixing steady and pulsating flow in a Y-junction provided with a ball valve [26]. This has been used to analyse the unsteady turbine performance for different waste-gate positions [27]. A similar design, with swappable disks controlled by variable speed electric motor was used to investigate about the influence of pulsating frequency, shape and peak amplitude on VGT turbine performance [19]. Although the original work was focused towards the study of cold pulsating flow, other research also demonstrated good modelling agreement when coupling with detailed heat transfer model [13]. In another experimental work to measure the turbine efficiency under pulsating flow, a pair of counter rotating plates have been used as a source of pressure pulsations [28].

In order to reproduce a flow that is more representative of an engine, a cylinder head can be utilized to generate flow pulses. In this design, air from the gas stand is fed into a large plenum that, in turn feeds a bespoke cylinder block that distributes the flow. Only the exhaust valve is utilized to create the pulsations from a constant pressure feed [29].

Whilst there are some similarities between the experimental facility in reference [29] and the pulsating device outlined in this paper, there are also a number of significant differences. The main difference is the demonstration in this paper of higher turbine inlet temperatures thanks to the uprated components (see section 4.1). The hot test facility is necessary as it important and useful to study the effect of turbine side heat transfer to oil, coolant and compressor [30], thrust load [31] and for high temperature mapping [32]. Also, hot tests are important if one wishes to load the turbine with its own compressor observing that ambient operation either results in a different speed parameter or a different compressor load range compared to normal turbocharger operation. It is thus important that if the turbine and compressor are to be studied together under pulsatile flow, that the pulse generator is capable of high-temperature operation. It is also designed with unique features such as an active valve train that are more characteristic of the modern internal combustion engine. As a direct result of these unique features, the facility described in this paper has been used to study the turbine and compressor unsteady behaviour in deactivated mode (2-cylinder mode) for the first time to the authors' knowledge.

2.1 TEST FACILITY OBJECTIVES

A standard radial turbo machinery gas stand utilizes steadystate flow conditions. However, in the particular application of a turbocharger, steady-state characterization is no longer sufficient. Thus, a pulsating flow generator is needed to re-create representative in-cylinder pulses at the turbine inlet in a controlled laboratory environment. This is important for:

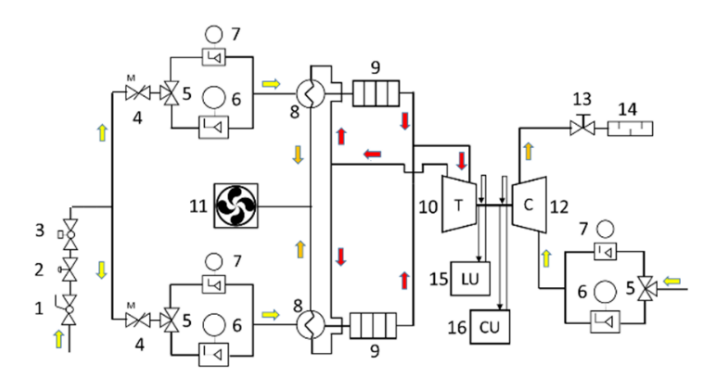
- Improved turbocharger turbine design
- Better modelling of the turbocharger-engine system
- Deeper understanding of the energy exchange due to variable valve actuation.

The final added value to consider is the greater understanding of the behaviour of the turbocharger when there is change in valve timing, lift or activation. Good examples are the divided exhaust period concept (DEP) [33] or cylinder deactivation where the valves are closed and the fuelling is cut off. The energy exchange to the turbine changes markedly as will be shown in an example data set out in this paper.

2.2 UNIVERSITY OF BATH TURBOCHARGER TEST FACILITY

It is important to briefly outline features of the turbocharger test stand at the University of Bath since this does inform some of the data and modelling presented in this paper. Figure 1 shows a schematic of the turbocharger test facility with the hot. electrically heated turbine supply and the compressor loading valve. The supply air is compressed externally to the test cell via two Ingersoll Rand compressors. The moisture or humidity is removed via Hankison refrigerated compressed air drier and therefore the air arriving at the test facility at ambient temperature and dry. The control of the mass flow rate of the supply air is achieved via a main ball valve and a pair of motorised gate valves installed on parallel pipework legs. Such a parallel arrangement of the pipework allows for testing of twin or double entry turbines. Each of the parallel supply air branches includes for two sizes of differential pressure V-cone mass flow meters to maintain measurement precision. After the mass flow measurement point the supply air gets through the recuperator/heat exchanger where it is heated up by the returning exhaust flow. Two electrical heaters deliver up to 88kW to the flowing air introduced to the turbine.

In the compressor side of the test facility, air is drawn from ambient upstream of the compressor and discharged against a valve after the compression process takes place. Similar to the turbine module, there are also two alternative mass flow measurement devices on the compressor side to maintain precision.



Number	Turbocharger gas stand equipment
1	Manual ball type shut off valve
2	SMC pneumatic pressure regulator
3	Ball type valve with Kinetrol electro-pneumatic positioner
4	Sierra CP motorized butterfly valve
5	Fiesto 3-way ball type valve
6	3" McCrometer V-cone mass flow meter with Siemens
0	DSIII differential pressure transmitter
7	2" McCrometer V-cone mass flow meter with Siemens
	DSIII differential pressure transmitter
8	Bowman gas-to-gas heat exchanger
9	Axes Design variable power electric heater
10	Turbocharger turbine
11	Electrically controlled roof extraction fan
12	Turbocharger compressor
13	Motorized backpressure valve
14	In-line type performance silencer
15	Turbocharger lubrication unit c/w variable speed pump, electric heater,
12	gas-to-water heat exchanger, pressure & temperature sensors
16	Turbocharger bearing housing cooling unit c/w electric heater,
10	water-to-water heat exchanger, temperature sensors

Figure 1. Layout of turbocharger gas stand facility

3. DESIGN METHODOLOGY AND CONCEPTION

The first intent of this paper is to discuss the approach adopted to design the pulsating flow generator, its principal components, and provide a comparison with the 1D gas-dynamic model used to design the device. This will also demonstrate the capabilities of the design should the reader wish to adopt a similar approach. The flow chart in Figure 2 shows the high level view of the methodology adopted to design the pulsation generator and to correlate its behaviour to the model.

There were two initial thoughts on the implementation. First, there was a desire to create a facility without piston movement as this significantly reduced the complexity of lubrication and cooling. Secondly, since there was to be no combustion, pressurized hot air must be added by the gas stand into the cylinders in some manner. There were two options here, feeding the hot air directly into the cylinder block as in reference [29] (by bypassing the cylinder head completely), or feeding it through the intake valves. After some initial exploratory modelling, it was concluded that allowing the intake valves to regulate the inflow of hot air into a fixed set of cylinders

produced pulse characteristics closest to the engine characteristics. This basic concept is shown in Figure 3.

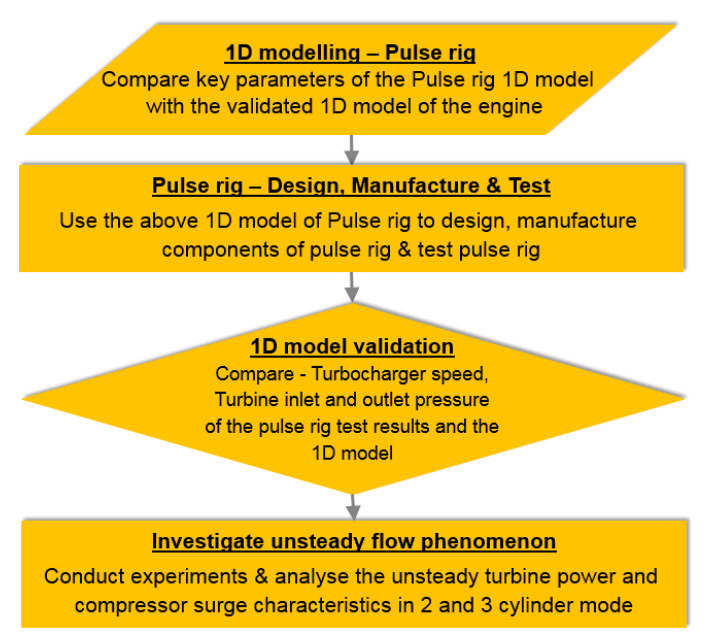


Figure 2 Flow chart of the methodology adopted for the design and testing of the pulsation generator

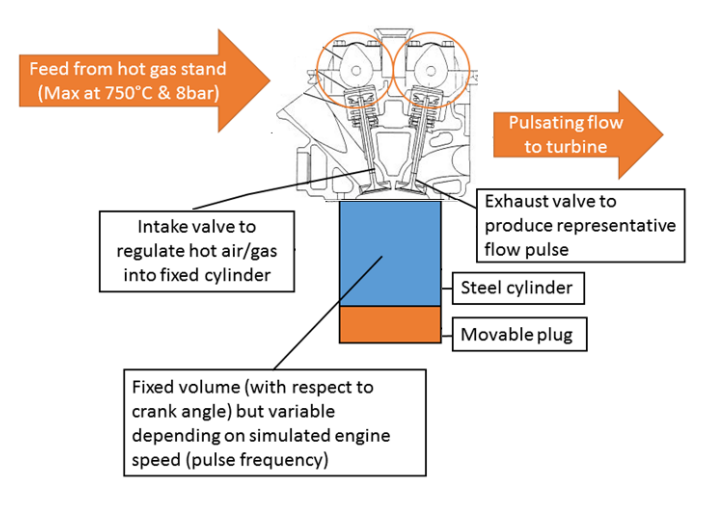


Figure 3 Basic schematic of the concept

3.1 ONE DIMENSIONAL MODELLING OF PULSATION GENERATOR

The one-dimensional (1D) gas dynamic modelling tool Ricardo Wave ® was used to produce the initial simulation results to feed into the detailed design of pulsation generator. This model of the pulsation unit was developed using the engine model corresponding to the cylinder head to be utilized and suppressing combustion [34]. The Woschni heat transfer submodel was used to calculate the heat transferred to and from the

charge assuming uniform heat flow coefficient and velocity as in Equation 1[15].

$$h_g = 0.0128 D^{-0.2} P^{0.8} T_c^{-0.53} V_c^{0.8} * C_{enht}$$
 Equation 1

Where, D = Cylinder bore

P = Cylinder pressure

 T_c = Cylinder temperature

 V_c = Characteristic velocity

Cenht = User-entered multiplier

Steady flow turbocharger performance maps were adopted in the 1D model assuming quasi-steady behaviour. The cylinder cooling sub model was modified to reflect the coolant and oil temperature of 80°C under test conditions. The, lift profiles for the intake and exhaust cams are maintained as shown in Figure 4. However, the valve timing (phasing) was modified to obtain the desired pressure profiles on the pulsation generator. In addition, the swept volume was allowed to be specified in the model (changed) so as to inform the final design.

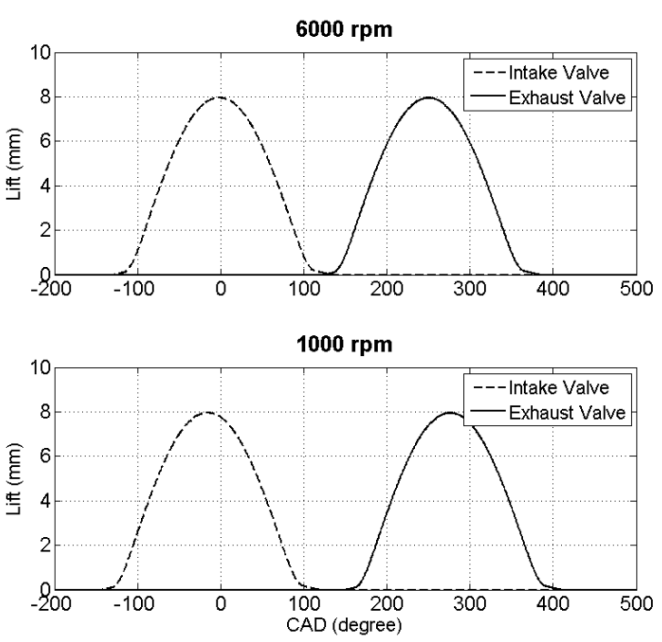


Figure 4 Inlet and Exhaust valve timings and profiles in the 1D model

The first major design decision was to understand if a change in fixed cylinder volume was needed from the base engine and whether this volume required a variation over the engine speed range. Figure 5 demonstrates that the variation in fixed cylinder volume starts at approximately the same value as the original engine at 1000 rpm and is required to double to achieve the best results at 6000rpm. These volumes were found to produce the best pressure profile match (between pulse generator and full engine models) with the resulting profiles shown in Figure 6. The simulation resulted in an average required engine displacement

of 1.731 for the entire operating range corresponding to a longer stroke with original 3 cylinders and bore as shown in Figure 5. A schematic of the 1D model is shown in Figure 8.

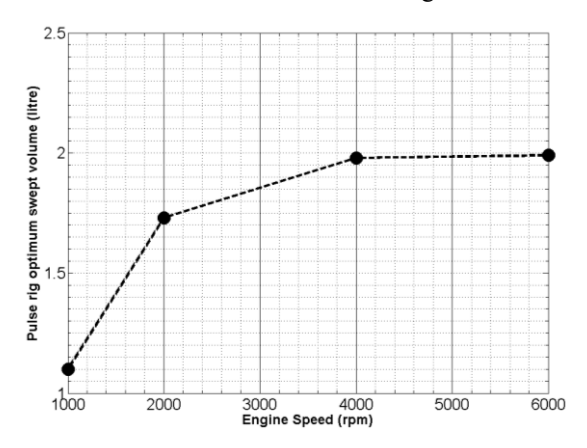


Figure 5 Pulsating flow generator optimum swept volume

Since the intent of this facility is to produce a good match to the characteristic pulse train of the original engine at the turbine inlet, a comparison was made between the pressure profile predicted from the model of the pulse generator and that from the original engine model in Figure 6. The magnitudes of the temperature pulses with the pulsating flow generator model, however, were predicted to be lower than the engine even though the pressure characteristics match well. If this was a combustor-fired facility, however, this would change the picture shown in Table 1 due to the higher temperature capability.

Table 1 Specification of the pulsation generator

Parameter	Value
No of cylinders	3
Bore	71.9 mm
Displacement (Variable)	1.732 litre

Thus, overall, the modelling work carried out in 1D simulation demonstrated that the concept of using a cylinder head fed by hot gas (air) from a steady-flow turbocharger test facility through the intake valves is able to produce a hot gas pulse train. What is more, it demonstrated that by feeding this hot air into the intake manifold from a gas stand, varying the intake cam phasing, and replacing the bottom end with a set of fixed volume cylinders, the resulting pulse shape resembled that which is seen from the engine.

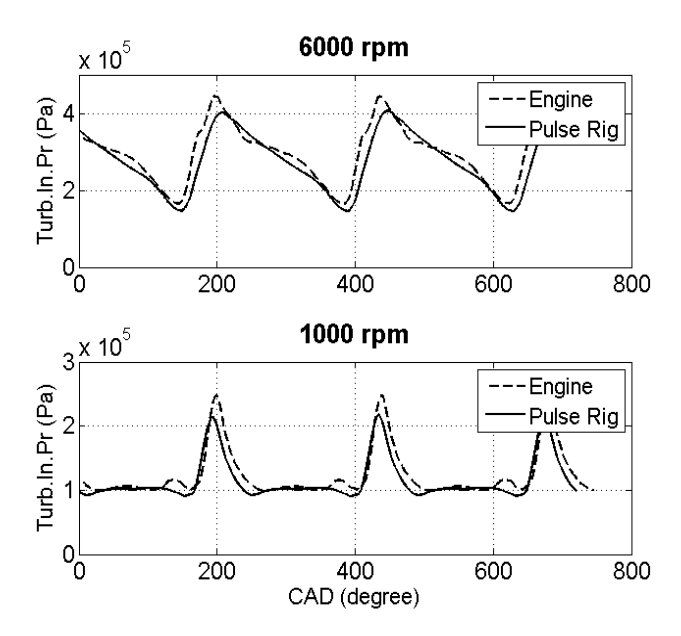


Figure 6 Comparing pressure pulses from 1D modelling - engine Vs Pulse rig

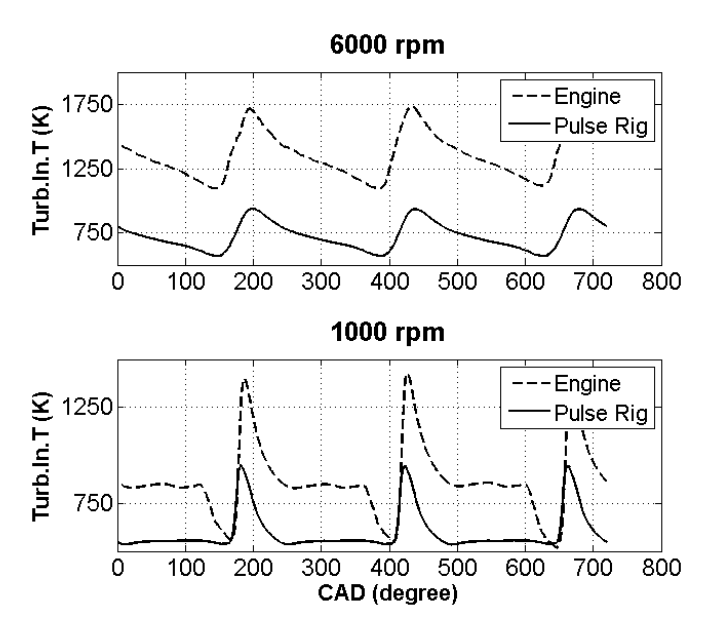


Figure 7 Temperature pulses - modelling comparison

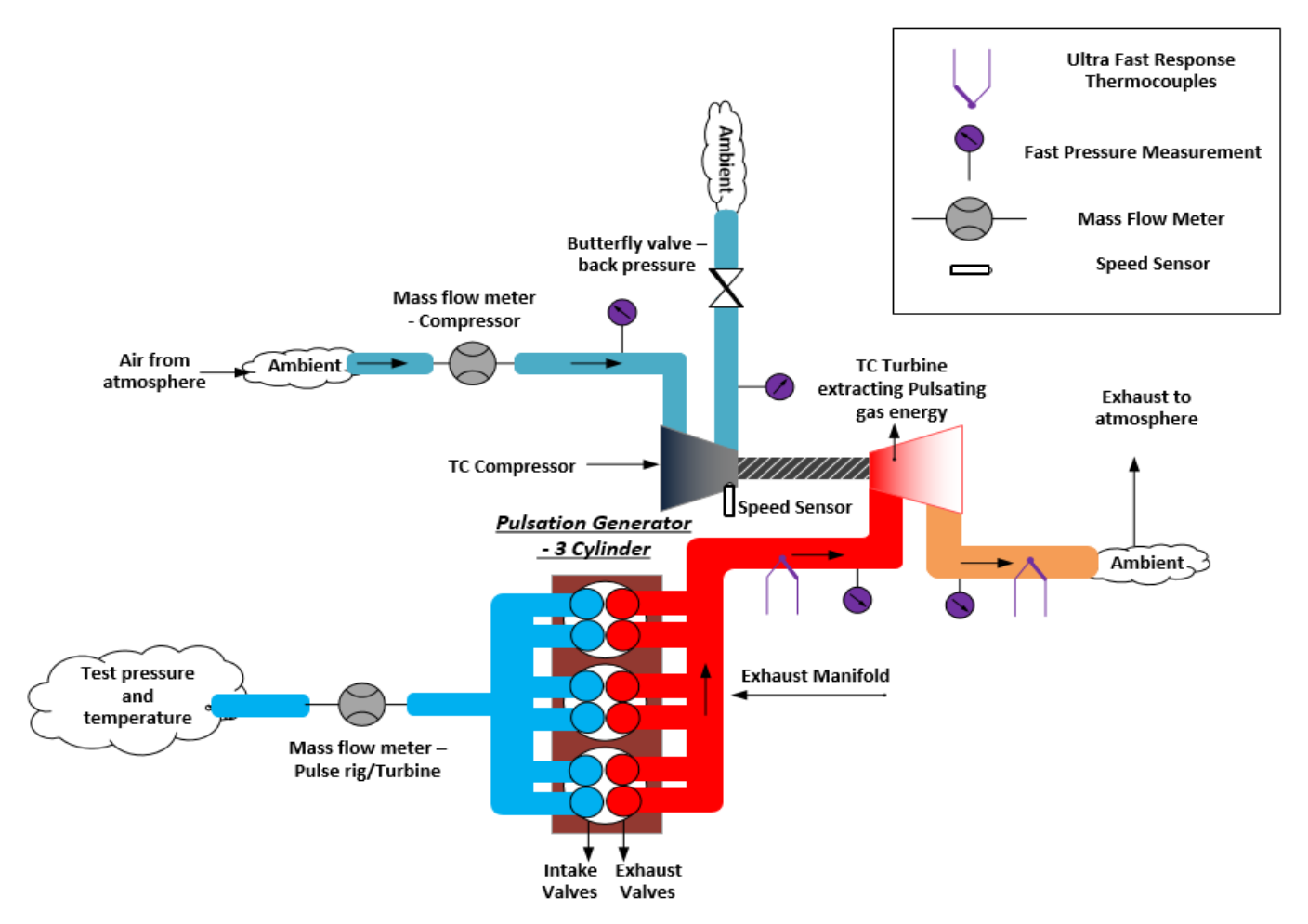


Figure 8 Schematic of the WAVE model of the Pulsation Generator

3.2 VALVE TIMING AND TURBINE OPERATION

Exhaust cam timing on the pulsation generator can be phased in relation to the intake cam shaft to vary the pulse amplitude. The effect of phasing on the amplitude of the pressure pulse is studied in the 1D model of the pulse generator by fixing the exhaust valve timing and sweeping the inlet valve timing as shown in Figure 9. This has the same effect on the turbine and compressor behaviour as phasing the exhaust cam with fixed intake cam timing since there is no piston/crank timing.

The boundary condition at the inlet of the pulse generator was set to 5 bar and 400°C with a pulse frequency corresponding to 1500 rpm engine speed. The opening of the compressor back pressure valve in the model was kept constant. As observed from Figure 10 the amplitude (and shape) of the pressure pulse changes significantly reaching ~4.5 bar at the highest point in the pulse and is strongly related to the overlap period between the valves.

Radial turbine efficiency is often plotted against the blade speed ratio (BSR) or velocity ratio. This parameter is defined as the ratio between the impeller tip speed (U) and the isentropic spouting velocity (C_{is}). This parameter provides 1D modelling codes a means to define the end points of the extrapolation curve fitted to the available data. Thus, there are two x-axis intercepts

at high and low velocity ratios that determine the shape of the curve and hence, the predicted off-design performance of the turbine. Figure 11 demonstrates how two different intercept settings in 1D code can produce extrapolation curves exhibiting significantly different behaviour. This is due to the lack of physics in the extrapolation and the limited data available from the steady-state gas stand loaded by a single compressor.

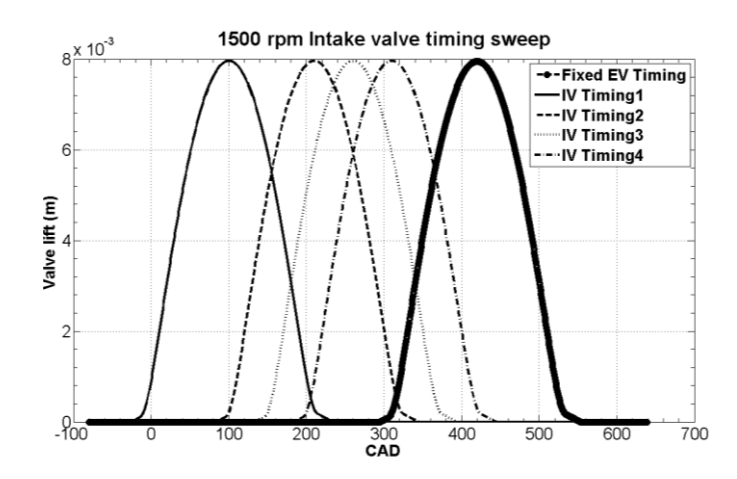


Figure 9 Intake valve timing sweep with fixed exhaust valve timing in 1D modelling (pulse generator)

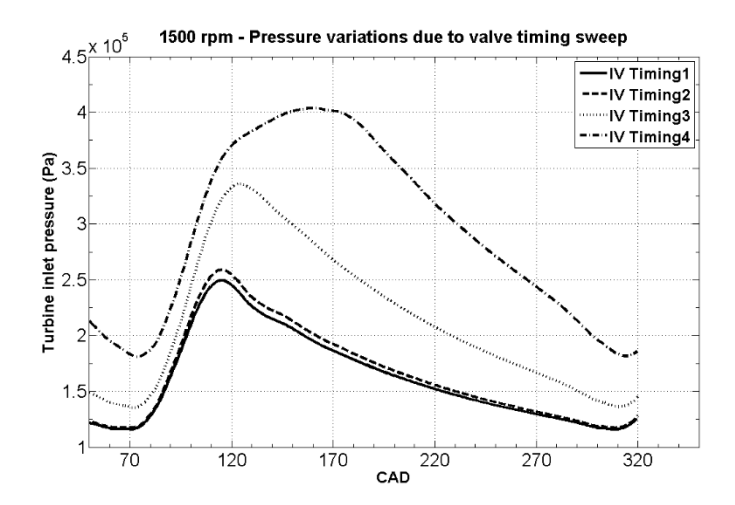


Figure 10 Variation in turbine inlet pressure with intake cam phasing at 1500 rpm

The question then can be posed: why is off-design turbine performance so important in a turbocharger? Figure 12 seeks to demonstrate this by showing the extent of turbine operation from a typical exhaust pulse as predicted by a 1D gas dynamic code. The red trace in this plot shows the instantaneous operation of a turbine resulting from the changes in exhaust temperature, mass flow and pressure. The prediction of this behaviour thus must heavily rely on the extrapolation of steady-state data.

There are two main approaches to improve the availability of off-design turbine data. The first is through methods to vary the turbine loading range in steady state gas stands. When loaded by a compressor, increased data range can be achieved through swapping to different compressor sizes [35], although this is time consuming and unrealistic for commercial mapping. The pressure at the inlet to the compressor can also be varied through the use of a closed loop that circulates the outlet air back to the inlet. Finally, the compressor can be replaced by a high-speed dynamometer [36] that produces a very broad range of turbine loads.

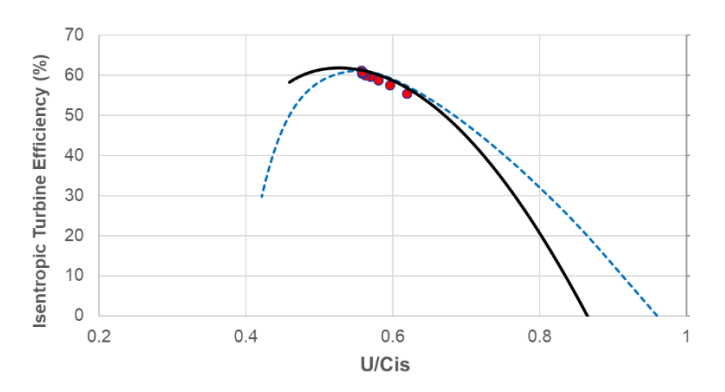


Figure 11 Turbine efficiency vs. Blade speed ratio.

Experimental steady state data (red points) with two example extrapolation curves

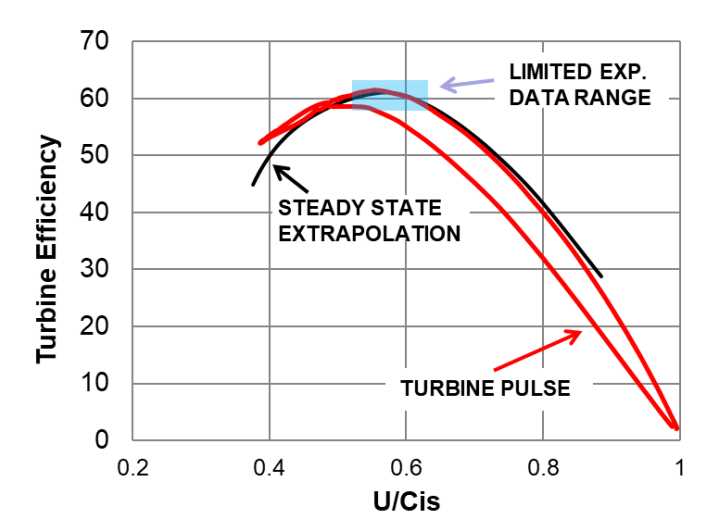


Figure 12 Turbine efficiency vs. Blade speed ratio. Extent of off-design operation during a typical exhaust pulse

The second approach to understand off-design turbine behaviour is to measure it during an exhaust pulse. Thus, the method proposed here is to use a complete turbocharger in a standard gas-stand set-up that uses a modified cylinder head to produce flow pulses. By measuring time-resolved quantities, off design turbine behaviour can be measured and quantified that both informs modelling tools, but also gives further insights into the interaction between the engine and the turbine. What is more, by measuring in a hot gas environment with a standard bearing housing, it negates the need for explicit friction and heat transfer models or corrections.

The model of the pulse generator was used to explore the limits of off-design data possible when valve overlap is varied. The instantaneous BSR and turbine efficiency based on zero overlap and maximum overlap between the inlet and exhaust valve cases compared to the steady flow values and the extrapolation curves are shown in Figure 13. The instantaneous points follow the extrapolation curves based on the user specified maximum BSR value.

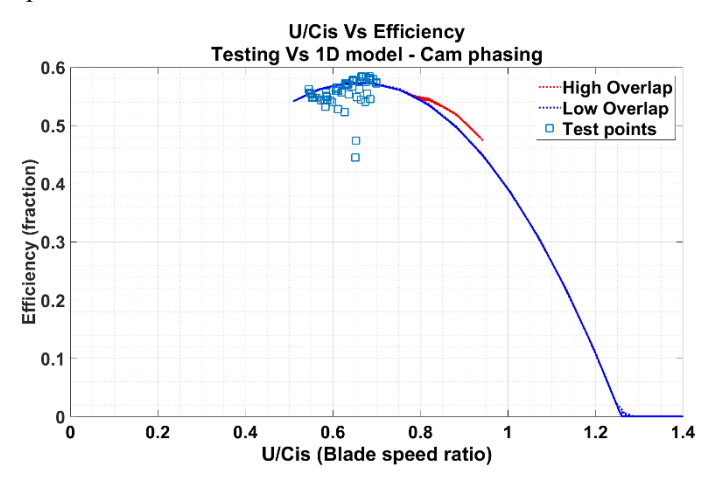


Figure 13 Turbine efficiency Vs Blade speed ratio – comparing steady flow map, 1D extrapolation and average values during phasing a pulse

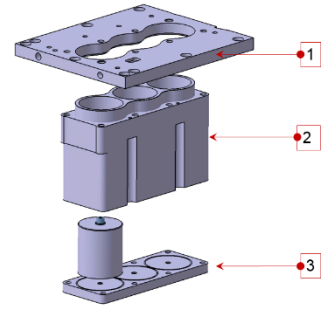
4. EXPERIMENTAL TEST FACILITY

4.1 PULSE GENERATOR HARDWARE DESIGN

The cylinder head components of the pulsation flow generator are designed primarily based on the 1D model of the pulsation generator mentioned above. Figure 14 shows the key components of the pulsation generator. Figure 15 and Figure 16 shows the isometric and cutaway views of the pulsation generator respectively with the constituting parts. Table 2 lists the component specifications of the pulsation generator.

Table 2 Components of the Pulsation Generator, specification/rating and material used

Component	Specification/ Rating	Material
Deck plate	-	Aluminium
Cylinder	-	Stainless Steel
Cylinder Sealing Plate	-	Stainless Steel
Front Cover	-	Aluminium
Drive Arrangement	22kW AC motor	-
Front Plate	-	Aluminium
Inlet Manifold	750°C and 8 bar	Stainless Steel
Side Plate	-	Aluminium
Intake & Exhaust Valves	450N/m	Engine exhaust grade



Deck plate
 Cylinder
 Drive arrangement
 Intake and Exhaust Valves

Cylinder sealing plate
 4. Front cove
 7. Side plate

9. Integrated Exhaust Manifold

Figure 14 Key Components of the Pulsation Flow Generator [37]

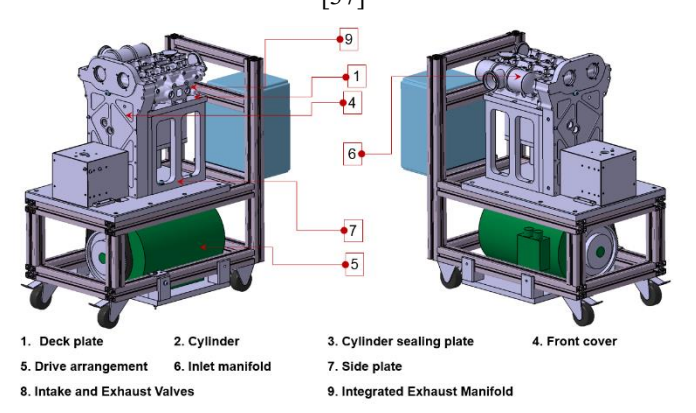


Figure 15 Isometric view of the pulsation flow generator [37]

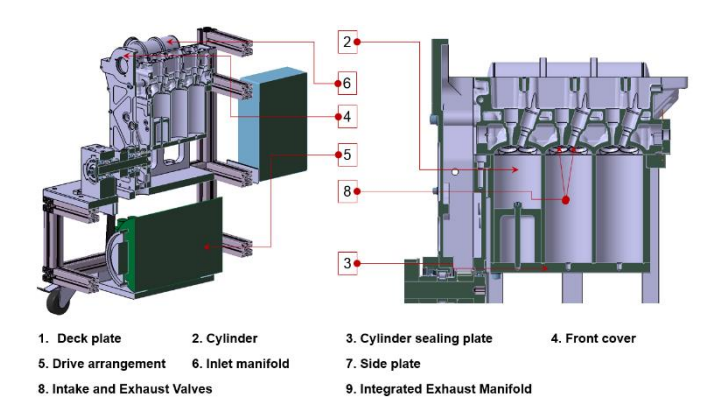


Figure 16 Cutaway view of the pulsation flow generator [37]

4.2 GAS-STAND PULSATING TEST FACILITY

The schematic of the experimental facility to test the steady flow and pulsation generator is shown in Figure 17. Compressed air up to a maximum pressure of 8 bar and 0.7 kg/s mass flow rate is fed from external compressors. After a set of control valves, the air goes through differential pressure V-cone mass flow meter and heaters capable of heating the air to 750°C at the turbine inlet. Air leaving the heater then passes through the inlet manifold of the pulsation generator, inlet valves, cylinder and the exhaust valves producing a pulsating flow at the turbine inlet.

The motor driving the cams was run at a speed corresponding to a specific engine condition. A temperature controlled oil system (Regloplas 300S) regulates lubricating oil supply for the intake and exhaust cam shafts. A standalone oil pump supplies oil to the turbocharger bearings. A temperature controlled water system (Regloplas 90 smart) was used to regulate the cylinder block temperature levels and to cool the turbocharger. Both Regloplas units were set to a fixed temperature of 80°C. A gate valve regulates backpressure at the compressor outlet and controls the compressor and turbine operating point.

4.3 MEASUREMENT AND DATA PROCESSING

The test facility is fitted with Sierra CP data acquisition system to record slow measurement (40 Hz) and Dewetron Sirius for fast measurements up to 100 kHz. The different type of sensors used, their accuracy, make/model, respective position on the facility and the measurement frequency are detailed in Table 3. The sampling frequency for the fast measurements specified in Table 3 is 10 kHz. A logging trigger signal is provided to Dewesoft from CP CADET to give the same start time to both systems.

The sensor positioning used for the experiment is shown in Figure 17. The static pressure was pneumatically averaged using four ports spaced at 90°. Similarly the average static temperature measurement used four thermocouples or PRT sensors spaced 90° apart at the measuring locations as specified in the SAE J1723 [9] and ASME PTC10 [38] gas stand code.

The unsteady compressor operating profile is based on the corrected mass flow rate and the TC speed over the duration of the pulse. The turbocharger speed recorded over the duration of the pulse was filtered using "sgolay" (moving average) curve

smoothing technique that does not phase shift the curve. The raw instantaneous turbine inlet and outlet pressure and filtered turbocharger speed for the duration of three-cylinder pulse from the facility are used in the comparison with the model for the

same compressor load (in model and testing). The instantaneous temperatures were measured using bespoke, ultra-fast response thermocouples to capture the smallest pulse detail.

Table 3 Sensor location, type, make, accuracy, and measurement frequency

Position/ Purpose of the sensor	Sensor type and Manufacturer/Model name	Accuracy / Resolution	Dewetron (10kHz) / CP (40 Hz)
Turbocharger speed	Eddy current – Micron Epsilon DZ135 sensor	FSO resolution of ±0.22%	Both
Turbine inlet and outlet static pressure	Water cooled Piezo-Resistive – Kistler sensors 4049B10DS1 and 4049A5s respectively	± 0.08% linearity of full scale output	Dewetron
Compressor inlet and outlet static pressure	Piezo resistive silicon elementPXM419- 3.5BAV and PXM419-002BGV	±0.08% FSO	Both
Air mass flow rate at the inlet of pulse generator	Siemens Sitrans P DSIII transmitter	± 0.51% FSO	СР
Average turbine inlet and outlet temperature	K Type thermocouples - TC Direct Pt100 (Precision)	± (0.15+0.002*t)	СР
Instantaneous turbine inlet and outlet temperature	K Type thermocouples (bespoke) - 13μm	10000 Hz	Dewetron

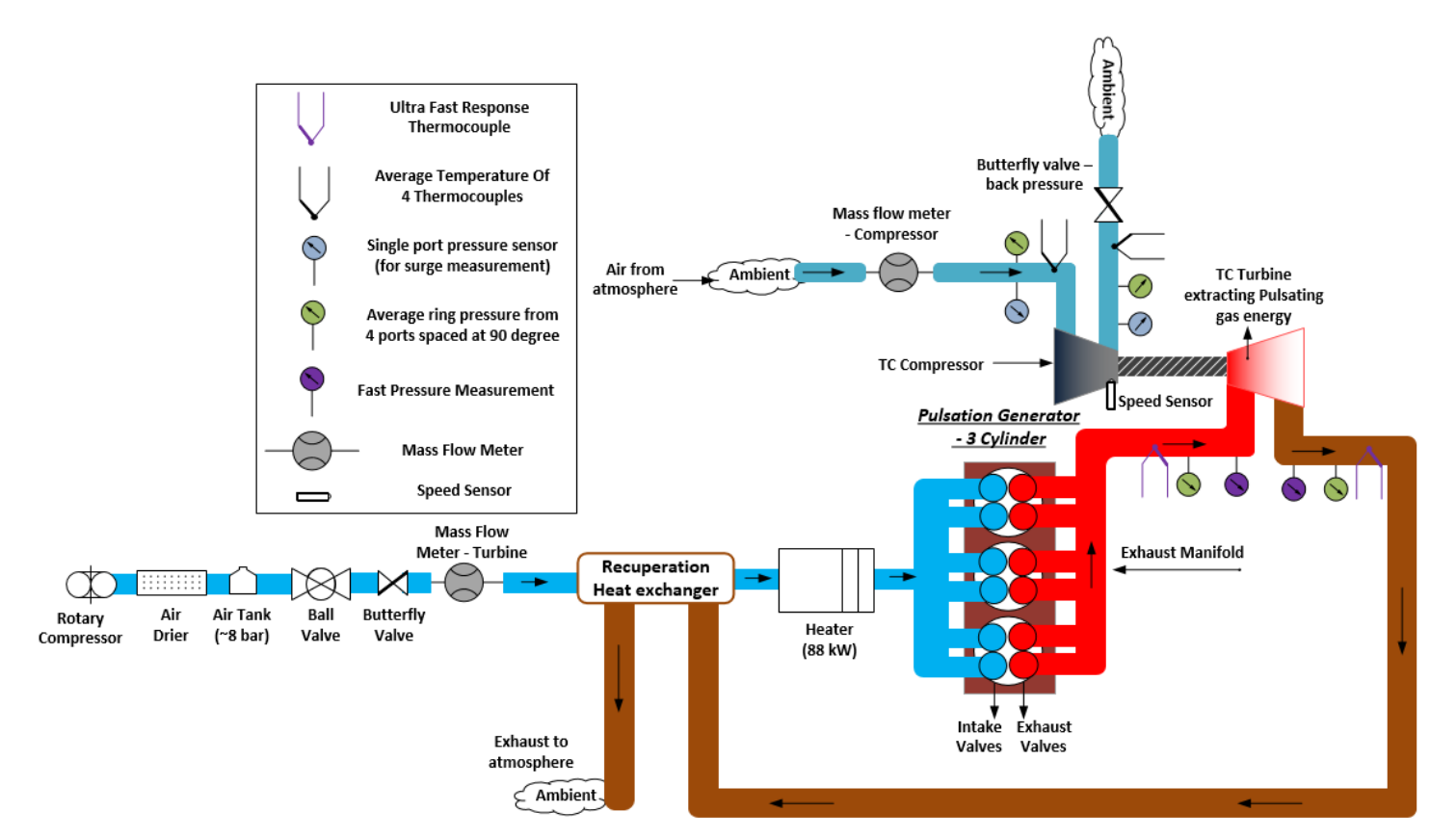


Figure 17 Schematic of the steady and pulsation flow generator experimental setup

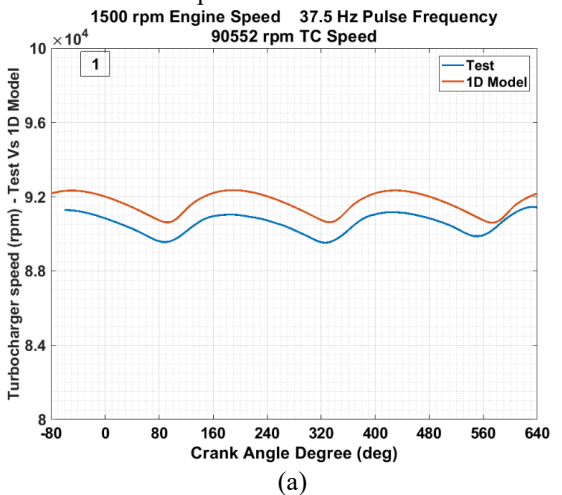
5. EXPERIMENTAL PULSE GENERATOR VS MODEL

The data in this section is simply to compare the results of initial experimental data to the model of the pulse facility to gauge agreement. The experiment was conducted on the pulsation flow generator discussed here with a prototype turbocharger (suitable for small automotive engine segment). The turbine integrated wastegate was kept completely shut throughout the tests.

5.1 TEST CASES

The position of the cylinder plug in the pulse generator was set to have a swept volume of 1.73 litres which is the best average position predicted from the 1D model. The time-averaged experimental conditions are provided in

Table 4. The pulse generator produced pulse frequencies between 37.5Hz and 57.5Hz corresponding to an engine speed range of 1500 to 2300rpm.



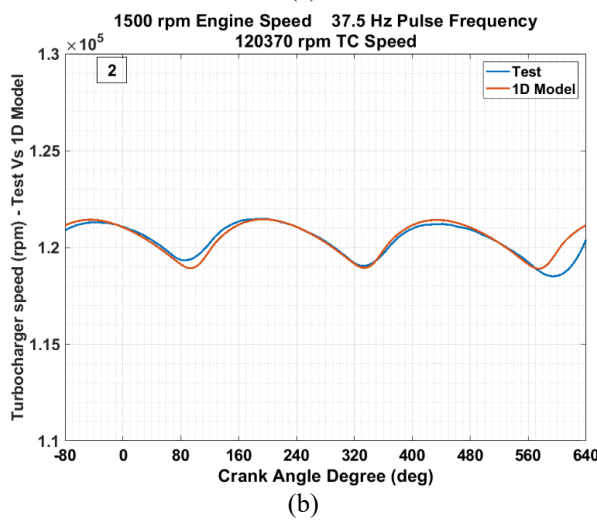


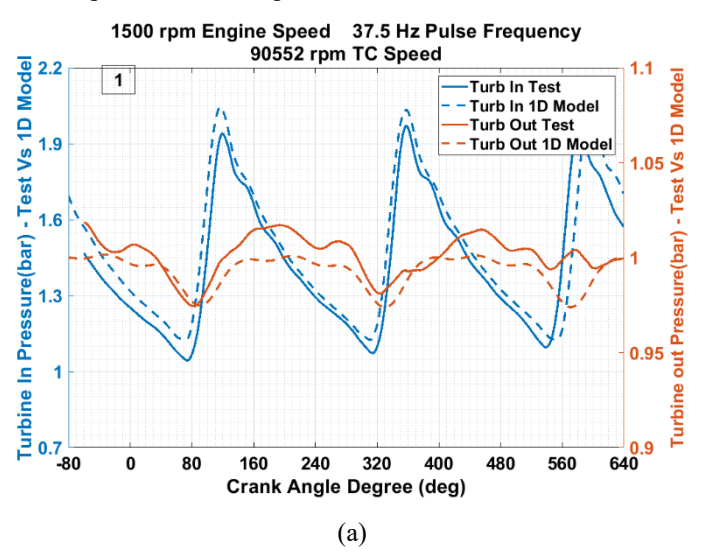
Figure 18 Instantaneous turbocharger speed comparison between the test and the 1D model of the pulsation generator

5.2 SAMPLE RESULTS AND MODEL COMPARISON

Three consecutive pulses from the experiment were compared to the 1D model of the pulse generator. The mass flow and pressure ratio across the compressor are within 5% of that

predicted from the 1D model when the same turbine load is maintained. The comparison of turbocharger speed with the 1D model is shown in Figure 18. The turbine inlet and outlet pressure of the pulse generator 1D model compares well with the test data as shown in Figure 19.

The use of very fine-wire thermocouples permitted the study of the dynamic temperature change at the turbine inlet. These thermocouples are bespoke units made for this specific measurement as shown in Figure 20. Two sizes were tested, namely $13\mu m$ and $25\mu m$, to check the response to pulsatile fluctuations. A smaller thermocouple can expect to exhibit faster response due to a smaller time constant. Figure 21 shows that the smaller 13 µm demonstrated a steeper rise and larger amplitude. To gain some confidence, this measurement was compared to the temperature profile that would result from an isentropic expansion and contraction of air as described by Equation 2. This procedure has been adopted by other researchers in the past [27, 28] and was demonstrated to be a valid assumption for a rotating valve pulse facility. As in that facility, Figure 21 shows that the assumption of isentropic expansion and contraction also matches very well to the 13µm fast-response thermocouple.



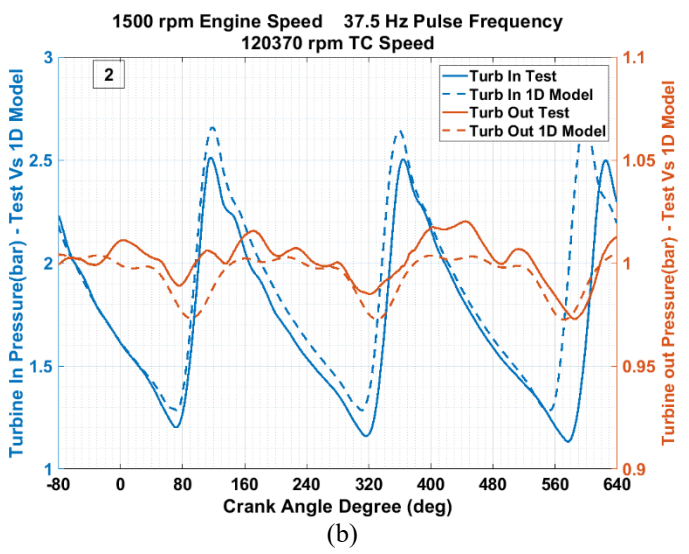
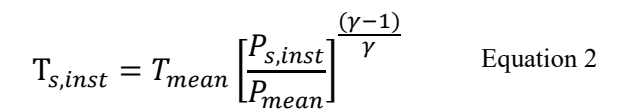
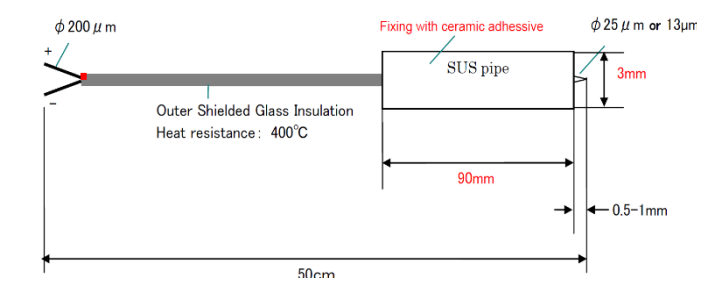


Figure 19 Instantaneous turbine inlet and outlet pressure comparison between test and 1D model of the pulse generator

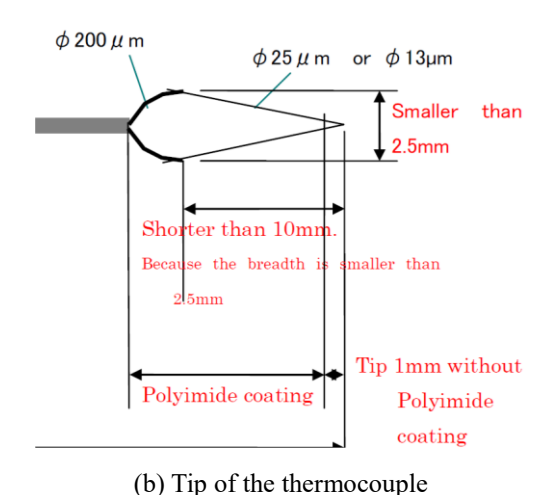
Table 4 Average data of ke	v test parameters	presented for pl	lots discussed	in this section
THE STATE OF THE STATE	j vest pontonine	presented for pr		***************************************

Test case	Engine speed	Average turbocharger speed	Average pulse rig inlet temperature	Average turbine pressure		tur	rage bine crature	Average comp. corrected MFR	Average comp. T-T pressure ratio
	(rpm)	(rpm)	(K)	Inlet (bar)	Outlet (bar)	Inlet (K)	Outlet (K)	(kg/s)	(-)
1	1500	90552	443	1.43	1	375.4	348.2	0.0353	1.137
2	1500	120370	453	1.73	1	382.9	343.7	0.0469	1.26
3	2300	142020	674.3	1.90	1	507.8	437.8	0.04	1.615





(a) Overall thermocouple



(b) The of the thermocouple

Figure 20: Ultra-fast response thermocouple

Figure 22 shows a comparison between the measured inlet fluctuating temperature (13 μ m thermocouple) and the isentropic assumption for a different pulse generator inlet temperature (180°C) and pulse frequency. As in Figure 21, this data also demonstrates a good agreement with the isentropic expansion/contraction calculation. However, the commercial 1D simulation model of the pulse facility did not match the

measured data seeing that the heat transfer model in the commercial code is designed to be used where there is combustion occurring and a large change in the direction of heat transfer during intake and exhaust in a real engine.

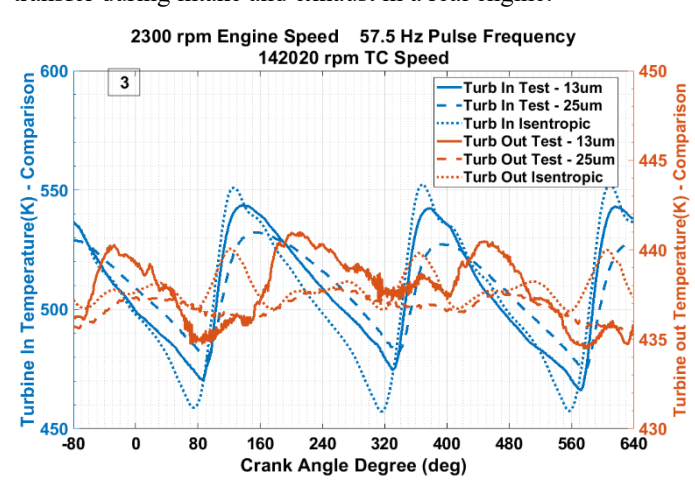


Figure 21: Temperature comparison at turbine inlet and outlet between 13 and 25 um and isentropic assumption

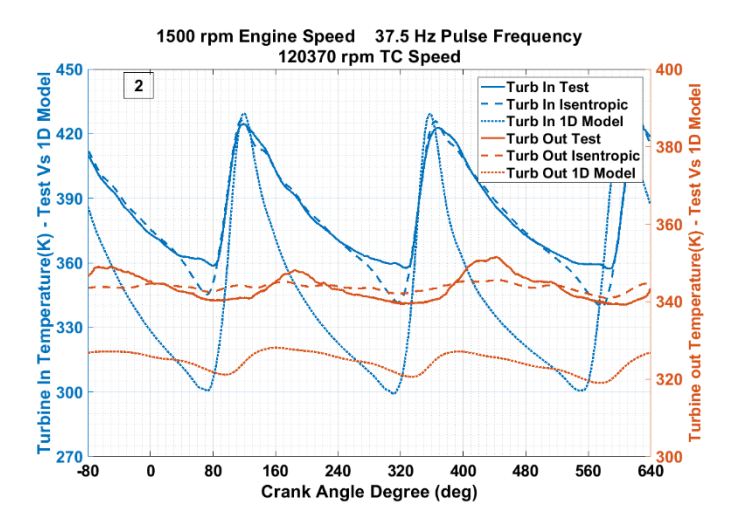


Figure 22 Instantaneous turbine inlet and outlet temperature comparison between the 1D model of the pulsation generator and the tests

In order to discuss the validity of the model of the pulse facility, the average mass flow measured from the v-cone meter shown in Figure 23 is compared with the modelled data. Figure 23 shows that the average mass flow rate from the initial experiment and 1D model of the pulse generator lies within 5% limits. The close match between the two shows that the calibration of the 1D model represents the hardware behaviour well on an average basis.

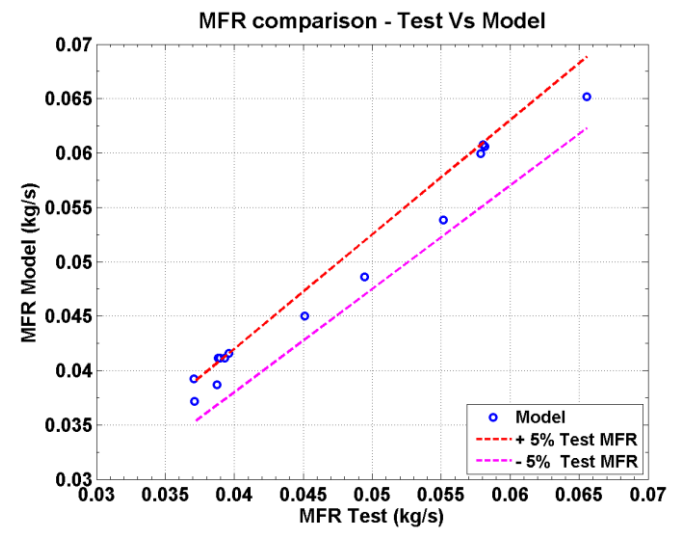


Figure 23 MFR comparison between test and 1D model at the pulsation generator inlet with $\pm 5\%$ margin

In conclusion, a pulse facility has been built and tested and demonstrated to be capable of producing hot pulsating flow from a cylinder head where a gas-stand feeds a redesigned intake system and cylinder volume. This provides confidence that the facility is fit for the purpose of recreating a realistic pulsatile flow at the turbocharger turbine characteristic of a modern internal combustion engine. By using the production cylinder head, one is able to explore the energy exchange to the turbine where there are changes in valve timing, lift or deactivation. In order to demonstrate some of these capabilities, the following sections will provide initial findings from two studies that will consider the influence of cylinder deactivation on turbine energy production and on compressor surge.

6. CYLINDER DEACTIVATION AND INFLUENCE ON THE TURBOCHARGER

6.1 ENERGY EXCHANGE TO THE TURBINE

Cylinder deactivation is seen as one of the means to improve the part load fuel savings of both diesel and gasoline engines [39]. Cylinder deactivation was achieved on the pulsation generator by simply blocking flow through one of the cylinders with a blanking plate at the inlet manifold. It is also referred to as 2-cylinder mode in this paper.

When a cylinder is deactivated on a running engine, the energy delivered to the turbine is reduced if nothing else is changed. This will, of course, result in a change in the turbocharger operating condition including a drop in its speed and boost level. However, since the compressor is decoupled from the engine in the current facility, we are able to explore the change in turbine inlet conditions that is required to maintain the same average compressor operating point (boost and speed) between the two and three cylinder modes.

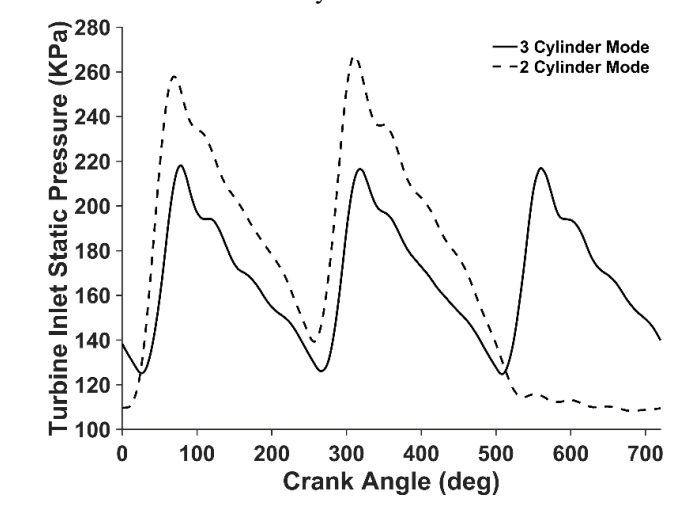


Figure 24 Instantaneous turbine inlet pressure comparison in test in 2 and 3 cylinder modes

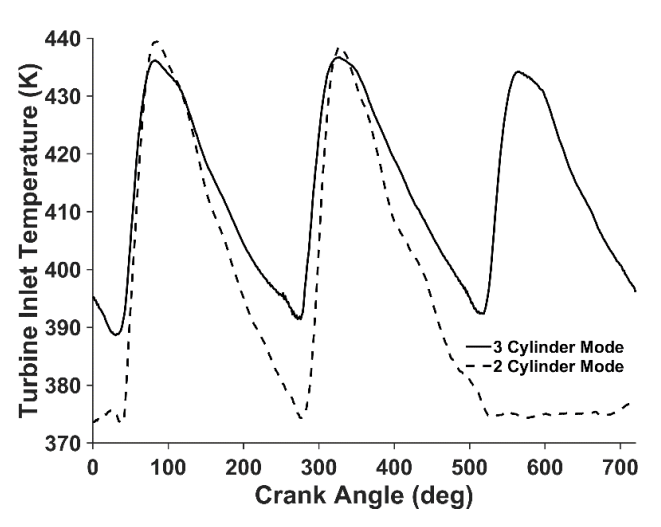


Figure 25 Instantaneous turbine inlet temperature comparison in test in 2 and 3 cylinder modes

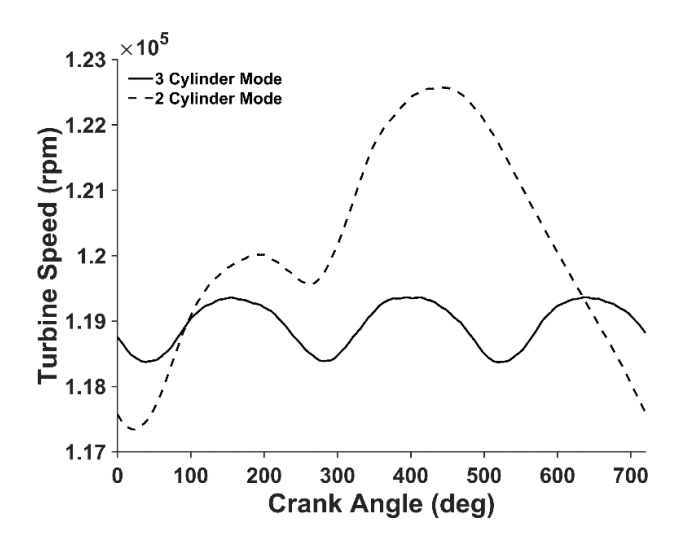


Figure 26 Instantaneous TC speed comparison in 2 cylinder mode and the test in 3 cylinder mode

Table 5 Average data of key test parameters for 2 Vs 3 cylinder mode comparison

Cylinder mode	Mean turbine inlet pressure	Mean turbine inlet temperature	Mean turbine outlet temperature	Mean TC speed	TC speed fluctuation	Turbine work in a cycle (J)		ycle (J)
	(kPa)	(K)	(K)	(rpm)	(rpm)	Positive work (J)	Negative work (J)	Total work (J)
2	169.36	393.2	352.7	119790	5718.3	89.3	-6.46	82.84
3	169.48	413	370.8	118950	1627.4	79.3	0	79.3

The change in turbine inlet conditions required to maintain approximately the same TC speed for the same average compressor load point is shown in Figure 24 to Figure 26. The average data during a full cycle (in 3 and 2 cylinder mode) is presented in Table 5. It is immediately clear from Figure 24 that in order to compensate for the missing pulse, the pressure amplitude in the two-cylinder mode increases substantially. The pressure amplitude and mean mass flow changes as shown in Figure 27 to deliver more turbine energy from two cylinders.

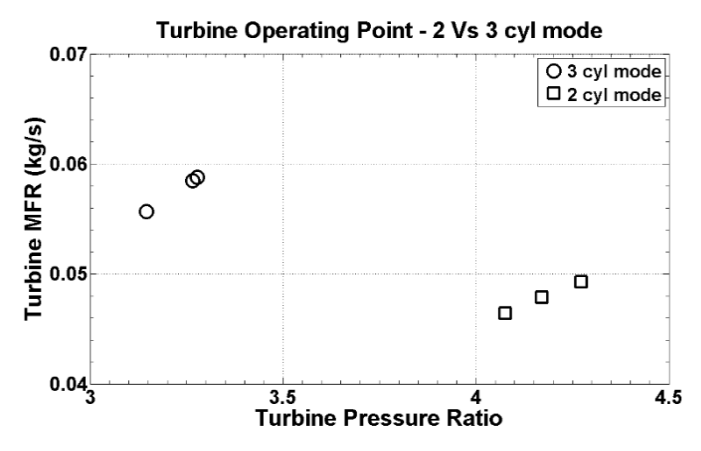


Figure 27 Average mass flow rate across the turbine in the pulsation generator test in 2 and 3 cylinder modes

Since the pressure, temperature and mass flow have all changed between the two and three cylinder modes whilst maintaining the same compressor operating point, it is more useful to compare on the basis of instantaneous turbine power. To do so, the fluctuating speed of the turbocharger can be used to derive power as outlined in Figure 28. This technique uses the compressor power to obtain the average shaft power and the fluctuating speed and inertia to obtain the unsteady (fluctuating) component of power. By adding these two together, a dynamic turbine power can be calculated from measured data. This technique has also been used by other researchers [27]. Helpfully, by using compressor power, the frictional power of the bearings is included in this derivation which is consistent with the industrial standard method of mapping turbines.

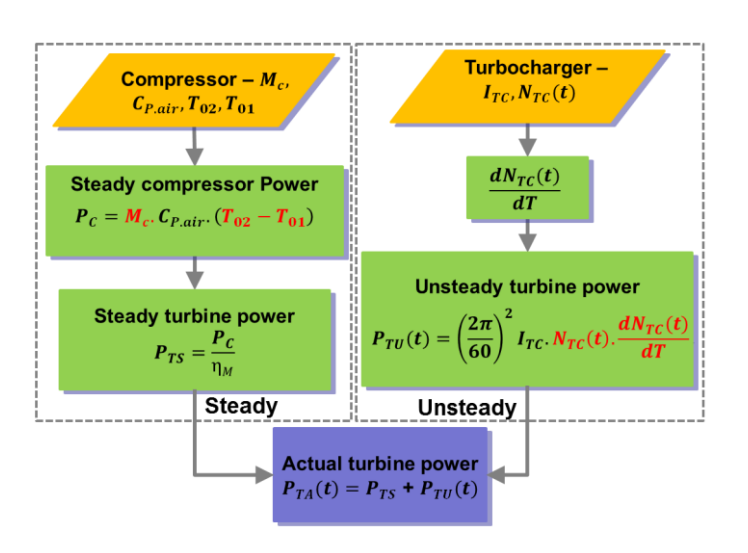


Figure 28 Steps involved in actual turbine power measurement

Figure 29 shows the difference in the instantaneous turbine power between the two and three-cylinder modes. As expected, when one cylinder is deactivated, the remaining two cylinders compensate to deliver much more peak power to the turbine in order to maintain the same compressor speed. This figure also shows another interesting feature of the turbine energy flow during two-cylinder mode. Deactivating a cylinder results in a gap in time where there is very little energy in the exhaust flow. Thus, there is a period where the inertia of the turbocharger continues to cause rotation, but where there is insufficient energy to support this. Hence, the turbine is 'free-wheeling' inducing a windage loss that translates into a large period of negative shaft power. It is also important to note that this type of data is impossible to gather using a steady-state gas stand since it is a purely transient phenomenon.

Section 3.2 discusses the importance of extrapolation of steady-state turbine data when modelling the behaviour of the turbine. Figure 30 shows the instantaneous variation in turbine velocity ratio that results from the pulsating flow during three-cylinder and two-cylinder operation. This clearly demonstrates that while a turbine on a gas stand may only experience a very limited range of conditions, when exposed to engine pulses, the turbine experiences a much broader flow regime. It also hints at a possible solution, namely to use the pulse facility to gather this off-design performance data to inform future modelling techniques [21].

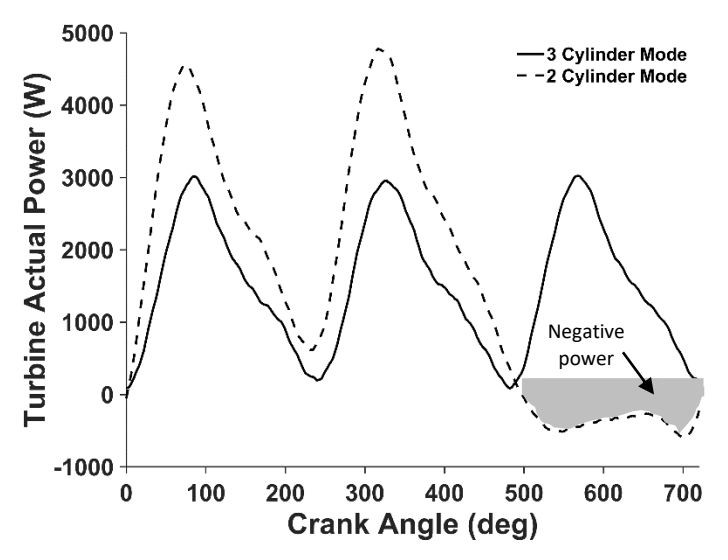


Figure 29 Instantaneous turbine power (including mechanical) from both three-cylinder and two-cylinder mode

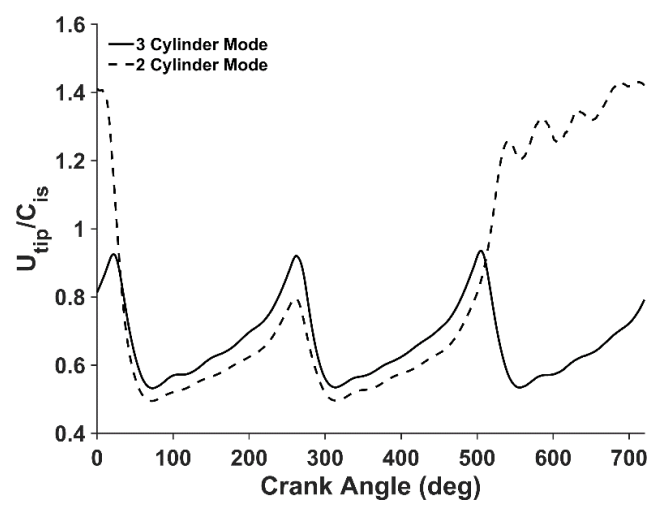


Figure 30 Variation in turbine blade speed ratio when exposed to a three-cylinder and two-cylinder pulses.

6.2 COMPRESSOR SURGE

A radial compressor is limited by compressor surge at low mass flow rates. Hard surge is characterized by severe flow reversal with audible coughing and banging [40] thus making it essential to avoid. If it is not avoided, compressor wheel damage and engine power fluctuation can result [41]. Thus, although it is important to operate close to the surge margin for maximum boost pressure especially for maximizing the low engine speed torque[42], it is essential to avoid surge for unpleasant user experience and component failure.

Compressor surge is normally measured under steady-state conditions on a gas stand when the performance map data is generated. However, it is well known that this approach can yield an inaccurate prediction of the location of surge. The difference between gas-stand measured surge and on-engine surge can be due to intake and exhaust pressure pulsation [43], aerodynamics in inducer[43], geometry of the inlet pipe [44], and variable valve actuation [45]. One of the key factors in surge, namely the influence of unsteady flow on the turbocharger, will be considered in this section with a particular focus on cylinder deactivation since to the authors' knowledge, no other work has considered this aspect.

An experimental study by Galindo et al. on a 6 cylinder diesel engine showed surge line improvement up to 15% (4 g/s) for 40-67 Hz pulse frequency range [43]. No significant link with pulse frequency was observed, however, the pulsation amplitude was found to linearly affect the surge margin improvement [43]. Importantly, the study showed a decrease in surge margin as the excitation frequency is brought close to surge frequency[43]. The results agree with the study by Marelli et al done on a cold pulse generator which also showed an early intake valve closure with a VVA moves the compressor operating point closer to the surge line [45].

There are two aspects to be presented here that add to the knowledge in this area of radial compressor surge research. First, unlike full engine testing, the pulsating flow facility is able to decouple the influence of turbocharger speed fluctuation with that of fluctuating pressure and mass flow through the compressor. Figure 17 demonstrates that the compressor is

controlled independently of the turbine with a backpressure valve. This helps to isolate any changes in surge as only being due to turbocharger speed fluctuation linked with pulsatile exhaust flow. The second aspect of surge to be presented here is the influence of cylinder deactivation. From the previous section, two-cylinder operation results in a much larger speed fluctuation that could influence the onset of surge.

Figure 31 shows the compressor map generated using steady state turbine flow. The red line that bounds the map on the left is the 'hard' surge point where completely unstable operation is found. From this 'hard' surge point, increasing the flow rate re-establishes stable operation, but is still characterized by pressure fluctuations and noise. The shaded area in the figure shows this area of mild or incipient surge.

The turbine was exposed to steady flow, unsteady threecylinder flow and finally, the flow with one cylinder deactivated. Since it is unlikely that two-cylinder operation will extend very far up the map, only the lowest two speed lines are considered here. In order to compare the surge behaviour, discrete points at constant speed were logged moving from a stable flow condition to hard surge in the mild surge region.

Figure 32a shows the location of hard surge for the first three speed lines where the turbine is exposed to pulsatile flow from all three cylinders under a range of pulse frequencies. Two conclusions can be drawn from this work. First, there is a small, but noticeable shift in the hard surge line to higher mass flows (10% to 21%) at low-mid turbocharger speed compared to the steady-state case. A marginal shift to lower mass flow (2 % to 10%) is observed at 142krpm. This is highly repeatable as evidenced by the repeated tests at different pulse generator frequencies as shown in Table 6. Secondly, there is only a very

small influence from the frequency of the pulsatile flow over the range considered. From this it can be broadly concluded that the turbine pulsations only provoke a minor change in the deep surge location.

However, interestingly, Figure 32b and Table 6 shows a more pronounced influence on the location of surge (29 % to 54 %) when exposed to two-cylinder pulses. Considering the much large speed variation shown in Figure 26, this is, perhaps, to be expected. What is more, there also is a larger change in the location of hard surge with a variation in the pulse frequency. More specifically, low pulse frequencies show a larger deviation from the steady-state behaviour.

The other item that is of interest is the mild or incipient surge behaviour. To assess this, a metric using downstream pressure amplitude has been selected. A high speed pressure transducer is placed in the compressor outlet pipe and the data in the mild surge region shown in Figure 31 is post-processed to calculate the peak-to-peak pressure fluctuating amplitude. The results from this study are shown in Figure 33. First consider the mild surge behaviour in the three-cylinder mode Figure 33 (a). This shows a small increase in the strength of mild surge when exposed to pulsating flow for 90 and 120krpm. However, this is relatively small and the 142krpm shows the opposite trend. Perhaps more interestingly, the two-cylinder mode Figure 33 (b) shows a much clearer rise in mild surge strength compared to the steady-state data. This confirms the general conclusion that the greater unsteadiness inherent in the two-cylinder pulse train result in both a shift in hard surge but also an increased intensity in the mild surge region. To the authors' knowledge, this is the first data published on the strength of surge during cylinder deactivation.

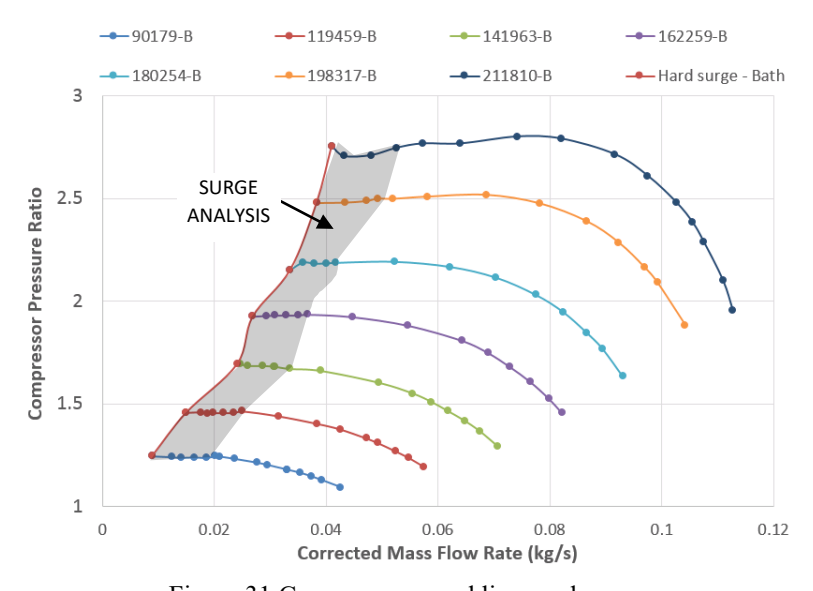


Figure 31 Compressor speed lines and surge area

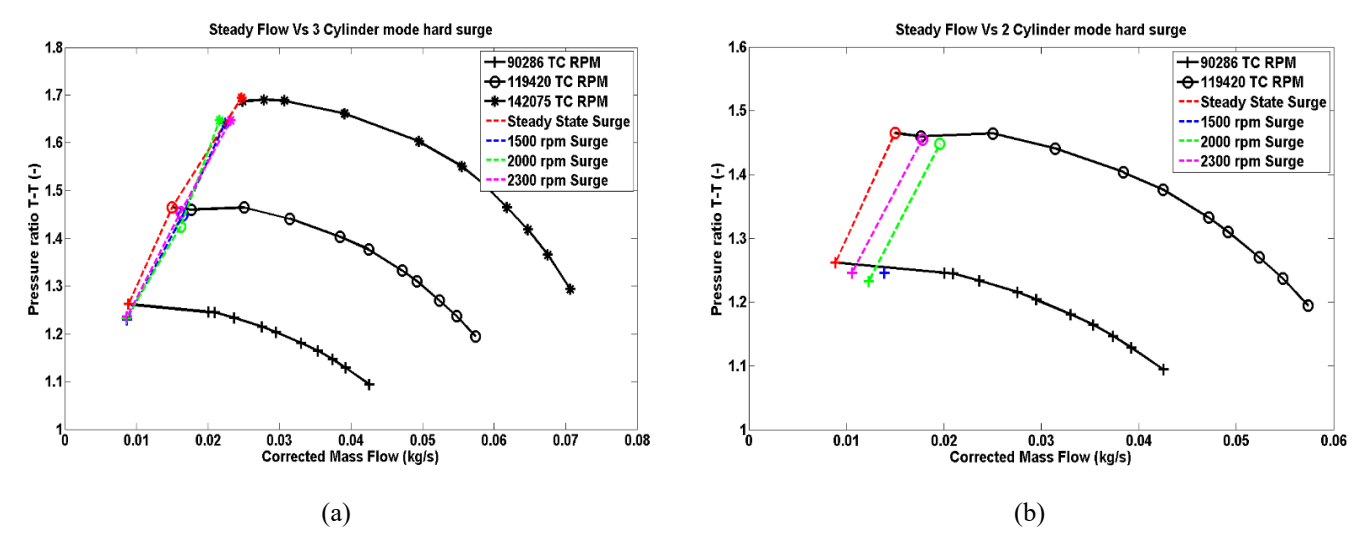
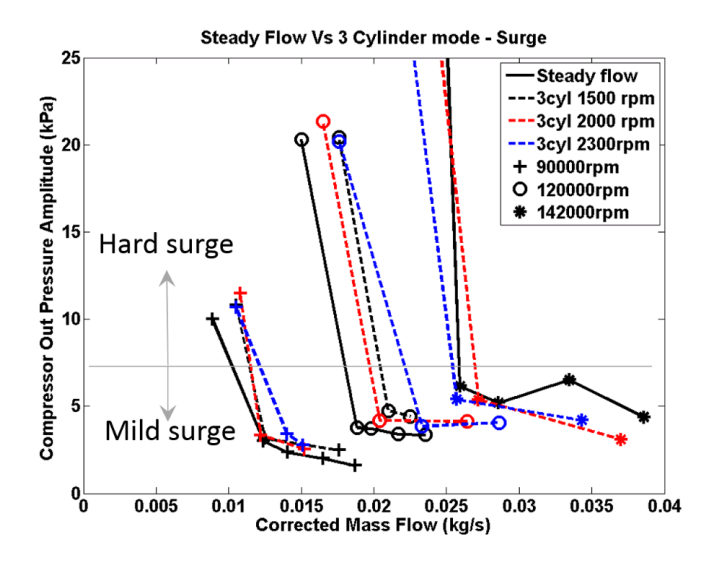
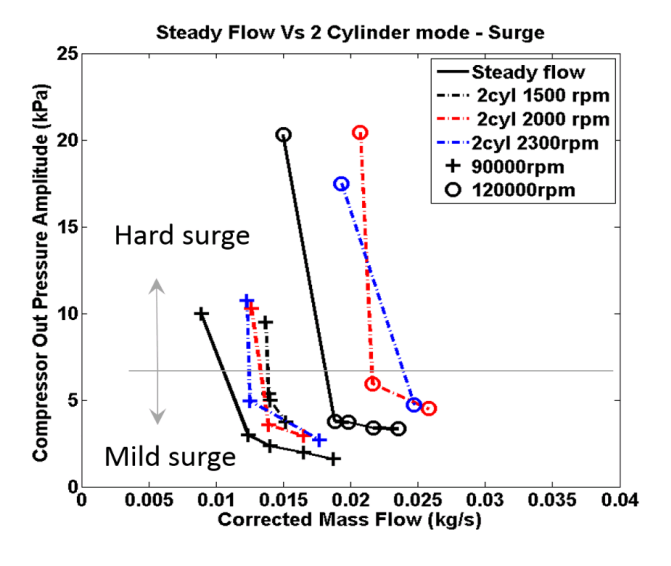


Figure 32 Compressor Hard Surge with the Turbine is exposed to (a) three-cylinder operation at various frequencies and (b) two-cylinder operation at various frequencies

Table 6 Summary of hard surge location in steady flow, 3 and 2 cylinder modes

Turbocharger speed (rpm)	Engine Speed Corresponding to the Pulse Frequency (rpm)	Percentage change in mass flow resulting in hard sur (pulsating – steady-state)		
(1 pm)	to the Tuise Frequency (Ipin)	3 Cyl mode	2 Cyl mode	
	1500	_+18 %	+54 %	
90000	2000	+21 %	+42 %	
	2300	+18 %	+38 %	
	1500	+17 %	-	
120000	2000	+10 %	38 %	
	2300	+17 %	29 %	
	1500	-3 %		
142000	2000	-2 %		
	2300	-10 %		





(a) (b)

Figure 33 Compressor surge strength in the form of (a) three-cylinder operation at various frequencies and (b) two-cylinder operation at various frequencies

7. CONCLUSION

The paper describes the steps involved in the design of a hot-gas pulsation flow generator and explains the various components of the test facility and the measurement system. The 1D model of the pulsation generator showed a wide range of turbocharger speed, turbine and compressor operating points achievable with the pulsation generator. Subsequently the hardware was designed maintaining the key engine features including the ability to vary valve timing.

Unsteady, instantaneous and time-averaged data was collected and plotted against that predicted by the 1D model of the pulse facility. This helped to validate the model that was used to show the projected capabilities of the system prior to build. It also gives confidence in using the 1D simulation to design experiments in the future. For the most part, the simulation tool was able to predict the behaviour in the laboratory using the pulsating generator.

The temperature measurements were made using a unique ultra-fine wire thermocouple. Whilst other authors have relied on fine wire anemometry, such probes are often incapable of the high turbine inlet temperatures that are the aim of this facility. This work, therefore, demonstrated the feasibility of this measurement. The fluctuating temperature data from this fine-wire thermocouple was compared to the isentropic expansion and contraction assumption that links pressure fluctuations to temperature. This comparison showed a good agreement that is in keeping with other researchers.

The final section of the paper considers two example experimental studies that are only possible using a pulsating generator. The first considers the change in pulsating energy transfer to the turbine that occurs when deactivating a single cylinder in a three-cylinder grouping. This work not only measured the required increase in unsteady power but also demonstrated that a large period of negative power is generated during the deactivated cylinder timing since the turbine is free-wheeling under its own inertia in a low energy exhaust flow. Moreover, the quantification of this negative power is *only* measurable using a pulsating generator and thus highlights a major weakness of 1D modelling that relies on steady-state mapping.

Another example provided to reinforce the use case of the facility is a small study that looks at the changes in surge behaviour over the lower parts of the compressor map as a result of turbocharger speed fluctuations. This removes any influence of intake pressure pulses (due to intake valve action) since the compressor is decoupled and develops pressure against a valve. Two new outcomes of this study are shown. First, the unsteady speed fluctuations result in a small but noticeable shift in the hard surge line to higher mass flows (10 % to 21 %) at low-mid turbocharger speeds and to marginally lower mass flow rates (2 % to 10 %) at 142krpm. This general behaviour is in agreement

with the other research published without cylinder deactivation [46].

The surge characteristic in 2 cylinder is different to 3 cylinder mode which has been shown in this paper for the first time to the authors' knowledge. The larger speed fluctuations resulting from the two-cylinder mode was expected to create more influence on surge that this was confirmed experimentally. The hard surge line moved to the right by 29 % to 54% when one cylinder was deactivated. In addition, there appeared to be a larger sensitivity to the frequency of the pulsations where lower frequencies resulting in a larger shift in the surge line. The mild surge behaviour was also shown to be influenced by cylinder deactivation. The relevance of these points to the importance in characterizing the location and strength of surge using a pulsating generator, especially where cylinder deactivation is employed. The current approach to characterizing surge using a steady-state gas stand will undoubtedly lead to incorrect modelling predictions and hence, component matching.

In conclusion, this paper summarizes a new type of pulsating flow generator design that is able to deliver representative hot pulses to the inlet of a turbocharger turbine in a controlled gas-stand laboratory environment. The research outcomes and knowledge based on the cylinder deactivation studies is applicable to internal combustion engines in different applications such as road transport, power generation and off road mining and construction. This will help to better model turbocharger behaviour leading to better component and system level optimization for energy efficiency. This will improve the sustainability of industries that continue to heavily rely on the internal combustion engine for propulsion or power generation.

ACKNOWLEDGMENTS

This work is a part of the Advanced Combustion Turbocharged Inline Variable valve train Engine (ACTIVE) project (Reference: 39215-287151) and was developed with the financial support from Advanced Propulsion Centre (APC). The authors would like to thanks Ford Dunton Technical Centre (UK), Continental Automotive Trading UK Ltd and all the Project Partners for their support.

NOMENCLATURE

1D One dimensional

BSR Blade Speed Ratio

Cenht User-entered multiplier

CFD Computational Fluid Dynamics

$C_{\rm is}$ or $C_{\rm o}$	Isentropic spouting velocity, m/s
$C_{P,air} \\$	Average specific heat at constant pressure of air
D	Cylinder bore
DEP	Divided Exhaust Period
$h_{\rm g}$	Heat flow coefficient
ICE	Internal Combustion Engine
I_{TC}	Turbocharger inertia, kg.m ²
$M_{\rm c}$	Air mass flow rate through the compressor, kg/s
$N_{TC}(t)$	Instantaneous turbocharger speed, rpm
P	Cylinder pressure
P_{c}	Compressor power, kW
P_{mean}	The average pressure during the pulse, N/m^2
$P_{s,inst} \\$	Instantaneous turbine inlet static pressure, N/m^2
$P_{TA}(t)$	Instantaneous actual turbine power, kW
P_{TS}	Steady turbine power, kW
$P_{TU}(t)$	Instantaneous unsteady turbine power, kW
SUS	Stainless steel
T_{01}	Compressor inlet total temperature
T_{02}	Compressor outlet total temperature
T_{c}	Cylinder temperature
TC	Turbocharger
$T_{\text{mean}} \\$	Average temperature during the pulse, K
$T_{s,inst} \\$	Instantaneous static turbine inlet temperature, K
U	Turbine tip speed, m/s
$V_{\rm c}$	Characteristic velocity
VGT	Variable Geometry Turbines
VNT	Variable Nozzle Turbines
VVA	Variable Valve Actuation

WG Waste Gate

 η_M Mechanical efficiency of the turbocharger

SUBSCRIPTS

mean Mean temperature or pressure during a pulses,inst Instantaneous static pressure or temperature

REFERENCES

- [1] Stokes J, Lake TH, Osborne RJ. A Gasoline Engine Concept for Improved Fuel Economy – The Lean Boost System. SAE Technical Paper 2000-01-2902, 2000. doi:10.4271/2000-01-2902.
- [2] Bandel W, Fraidl GK, Kapus PE, Sikinger H, Cowland CN. The Turbocharged GDI Engine: Boosted Synergies for High Fuel Economy Plus Ultra-low Emission. SAE Technical Paper 2006-01-1266, 2006. doi:10.4271/2006-01-1266.
- [3] Feneley AJ, Pesiridis A, Andwari AM. Variable Geometry Turbocharger Technologies for Exhaust Energy Recovery and Boosting-A Review. Renewable and Sustainable Energy Reviews 2017;71:959–75. doi:10.1016/J.RSER.2016.12.125.
- [4] Serrano JR, Arnau FJ, Dolz V, Tiseira A, Lejeune M, Auffret N. Analysis of the Capabilities of a Two-stage Turbocharging System to Fulfil the US2007 Anti-pollution Directive for Heavy Duty Diesel Engine. International Journal of Automotive Technology 2008;9:277–88. doi:10.1007/s12239-008-0034-5.
- [5] Martinez-botas R, Pesiridis A, Mingyang Y.
 Overview of Boosting Options for Future
 Downsized Engines. Science China 2011;54:318–31. doi:10.1007/s11431-010-4272-1.
- [6] King J, Barker L, Martin J, Turner J. SuperGen -A Novel Low Cost Electro-Mechanical Mild Hybrid and Boosting System for Engine Efficiency Enhancements. SAE Technical Paper 2016-01-0682, 2016. doi:10.4271/2016-01-0682.
- [7] Mamat AMI, Romagnoli A, Martinez-Botas RF. Characterisation of a Low Pressure Turbine for Turbocompounding Applications in a Heavily Downsized Mild-hybrid Gasoline Engine. Energy 2014;64:3–16. doi:10.1016/j.energy.2012.09.064.
- [8] Martin G, Talon V, Higelin P, Charlet A, Caillol C. Implementing Turbomachinery Physics into Data Map-Based Turbocharger Models. SAE International Journal of Engines 2009;2:211–29. doi:10.4271/2009-01-0310.

- [9] SAE_J1723. Supercharger testing standard. SAE International, 1995, p. 1–9. doi:J1723_199508.
- [10] Copeland CD, Martinez-Botas R, Seiler M.
 Comparison Between Steady and Unsteady
 Double-Entry Turbine Performance Using the
 Quasi-Steady Assumption. ASME Turbo Expo:
 Power for Land, Sea, and Air, Volume 7:
 Turbomachinery, Parts A and B 2009;7:1203–12.
 doi:10.1115/GT2009-59290.
- [11] Hellstrom F, Renberg U, Westin F, Fuchs L. Predictions of the Performance of a Radial Turbine with Different Modeling Approaches: Comparison of the Results from 1-D and 3-D CFD. SAE Technical Paper 2010-01-1223, 2010. doi:10.4271/2010-01-1223.
- [12] Hadef J El, Colin G, Chamaillard Y, Talon V. Physical-Based Algorithms for Interpolation and Extrapolation of Turbocharger Data Maps. SAE International Journal of Engines 2012;5:363–78. doi:10.4271/2012-01-0434.
- [13] Serrano JR, Arnau FJ, Novella R, Reyes-Belmonte M. A Procedure to Achieve 1D Predictive Modeling of Turbochargers under Hot and Pulsating Flow Conditions at the Turbine Inlet. SAE Technical Paper 2014-01-1080 2014. doi:10.4271/2014-01-1080.
- [14] WAVE_Manual. WAVE manual Turbine Panel: Menu Bar: Run Menu: Map Processing. Shoreham-by-Sea: 2016.
- [15] GT_SUITE. User's Manual and Tutorial, GT-SUITETM Version 7.5.0 Build 2. 2016.
- [16] Moraal P, Kolmanovsky I. Turbocharger Modeling for Automotive Control Applications. SAE Technical Paper 1999-01-0908, 1999. doi:10.4271/1999-01-0908.
- [17] Reyes-Belmonte MA. Contribution to the Experimental Characterization and 1-D Modelling of Turbochargers for IC Engines. Doctoral Thesis. Universitat Politècnica De València, 2013. doi:10.4995/Thesis/10251/34777.
- [18] Payri F, Serrano JR, Fajardo P, Reyes-Belmonte MA, Gozalbo-Belles R. A Physically Based Methodology to Extrapolate Performance Maps of Radial Turbines. Energy Conversion and Management 2012;55:149–63. doi:10.1016/j.enconman.2011.11.003.
- [19] Serrano JR, Arnau FJ, Fajardo P, Reyes-Belmonte MA, Vidal F. Contribution to the Modeling and

- Understanding of Cold Pulsating Flow Influence in the Efficiency of Small Radial Turbines for Turbochargers. ASME J Eng Gas Turbines Power 2012;134:102701–11. doi:10.1115/1.4007027.
- [20] Rehnberg U, Ångström H, Olofsson U. Instantaneous On-Engine Turbine Efficiency for an SI Engine in the Closed Waste Gate Region for 2 Different Turbochargers. SAE Technical Paper 2006-01-3389 2006. doi:https://doi.org/10.4271/2006-01-3389.
- [21] Liu Z, Copeland C. New method for mapping radial turbines exposed to pulsating flows. Energy 2018;162:1205–22. doi:10.1016/j.energy.2018.08.107.
- [22] Wallace FJ, Adgey JM, Blair GP. Performance of Inward Radial Flow Turbines Under Non-steady Flow Conditions. Proceedings of the Institution of Mechanical Engineers 1970;185:1091–105. doi:10.1243/PIME_PROC_1969_184_017_02.
- [23] Benson RS. Nonsteady Flow in a Turbocharger Nozzleless Radial Gas Turbine. SAE Technical Paper 740739, 1974. doi:https://doi.org/10.4271/740739.
- [24] Capobianco M, Marelli S. Turbocharger Turbine Performance Under Steady and Unsteady Flow: Test Bed Analysis and Correlation Criteria. 8th International Conference on Turbochargers and Turbocharging, Woodhead Publishing Limited; 2006, p. 193–206. doi:https://doi.org/10.1016/B978-1-84569-174-5.50018-X.
- [25] Luján JM, Bermúdez V, Serrano JR, Cervelló C. Test Bench for Turbocharger Groups Characterization. SAE Technical Paper 2002-01-0163 2002. doi:https://doi.org/10.4271/2002-01-0163.
- [26] Piscaglia F, Onorati A, Marelli S, Capobianco M. Unsteady Behavior in Turbocharger Turbines: Experimental Analysis and Numerical Simulation. SAE Technical Paper 2007-24-0081, SAE International; 2007. doi:https://doi.org/10.4271/2007-24-0081.
- [27] Capobianco M, Marelli S. Experimental analysis of unsteady flow performance in an automotive turbocharger turbine fitted with a waste-gate valve. Proceedings of the Institution of Mechanical Engineers, Part D: Journal of Automobile Engineering 2011;225:1087–97. doi:https://doi.org/10.1177/0954407011403369.

- [28] Szymko S, Martinez-Botas RF, Pullen KR. Experimental evalation of turbocharger turbine performance under pulsating flow conditions. ASME Turbo Expo 2005: Power for Land, Sea, and Air 2005;6:1447–57. doi:10.1115/GT2005-68878.
- [29] Capobianco M, Marelli S. Unsteady Flow Turbine Performance in Turbocharged Automotive Engines. 11th EAEC European Automotive Congress, Budapest, Hungary: GTE; 2007, p. 1– 16.
- [30] Schinnerl M, Ehrhard J, Bogner M, Seume J. Correcting Turbocharger Performance Measurements for Heat Transfer and Friction. Journal of Engineering for Gas Turbines and Power 2017;140:022301. doi:10.1115/1.4037586.
- [31] Hoepke B, Uhlmann T, Pischinger S, Lueddecke B, Filsinger D. Analysis of Thrust Bearing Impact on Friction Losses in Automotive Turbochargers. Journal of Engineering for Gas Turbines and Power 2015;137. doi:10.1115/1.4029481.
- [32] Serrano JR, Olmeda P, Arnau FJ, Dombrovsky A, Smith L. Analysis and Methodology to Characterize Heat Transfer Phenomena in Automotive Turbochargers. Journal of Engineering for Gas Turbines and Power 2014;137. doi:10.1115/1.4028261.
- [33] Hu B, Akehurst S, Brace C, Copeland C, Turner J. 1-D Simulation Study of Divided Exhaust Period for a Highly Downsized Turbocharged SI Engine Scavenge Valve Optimization. SAE International Journal of Engines 2014;7:1443–52. doi:https://doi.org/10.4271/2014-01-1656.
- [34] WAVE_Manual. Using WaveBuild: Menu Bar: Model Menu. Shoreham-by-Sea: 2016.
- [35] Scrimshaw KH. Scale Effects in Small Geometrically Similar Radial Gas Turbines with Particular Reference to Bladeless Volute Phenomena. PhD Thesis. University of London, 1981.
- [36] Szymko S, McGlashan NR, Martinez-Botas R, Pullen KR. The Development of a Dynamometer for Torque Measurement of Automotive Turbocharger Turbines. Proceedings of the Institution of Mechanical Engineers, Part D: Journal of Automobile Engineering 2007;221:225–39. doi:https://doi.org/10.1243/09544070JAUTO401.
- [37] Copeland C, Capon G, Witt D, Akehurst S. A

- Novel Pulse Generator for Turbocharger Gas Stand Application. 83605987, 2015.
- [38] ASME_PTC10-1997. Performance Test Code on Compressors and Exhausters. New York: 1997.
- [39] Zammit J, Mcghee MJ, Shayler PJ, Pegg I. The Influence of Cylinder Deactivation on the Emissions and Fuel Economy of a Four-Cylinder Direct-Injection Diesel Engine. Proceedings of the Institution of Mechanical Engineers, Part D: Journal of Automobile Engineering 2014;228:206–17. doi:https://doi.org/10.1177/0954407013506182.
- [40] SAE_J922. Turbocharger Nomenclature and Terminology. United States: 1995.
- [41] Kerres B. On Stability and Surge in Turbocharger Compressors. PhD Thesis. KTH Royal Institute of Technology, 2017.
- [42] Bellis V De, Bozza F, Marelli S, Capobianco M. Experimental Investigation and 1D Simulation of a Turbocharger Compressor Close to Surge Operation. SAE International Journal of Engines 2015;8:1866–78. doi:https://doi.org/10.4271/2015-01-1720.
- [43] Galindo J, Climent H, Guardiola C, Tiseira A. On the Effect of Pulsating Flow on Surge Margin of Small Centrifugal Compressors for Automotive Engines. Experimental Thermal and Fluid Science 2009;33:1163–71. doi:https://doi.org/10.1016/j.expthermflusci.2009. 07.006.
- [44] Galindo J, Tiseira A, Navarro R, Tarí D, Meano CM. Effect of the Inlet Geometry on Performance, Surge margin and Noise Emission of an Automotive Turbocharger Compressor. Applied Thermal Engineering 2017;110:875–82. doi:https://doi.org/10.1016/j.applthermaleng.2016.08.099.
- [45] Marelli S, Capobianco M, Zamboni G. Pulsating Flow Performance of a Turbocharger Compressor for Automotive Application. International Journal of Heat and Fluid Flow 2014;45:158–65. doi:https://doi.org/10.1016/j.ijheatfluidflow.2013. 11.001.
- [46] Avola C, Copeland C, Duda T, Burke R.
 Compressor Surge for Fully and Semi Fluctuating
 Flows in Automtoive Turbochargers. Proceedings
 of the 1st Global Power and Propulsion Forum,
 GPPS, Zurich, Switzerland: Global Power and
 Propulsion Society; 2017, p. 1–9.